Proceedings of the XVII ECSMGE-2019
Geotechnical Engineering foundation of the future
ISBN 978-9935-9436-1-3
© The authors and IGS: All rights reserved, 2019
doi: 10.32075/17ECSMGE-2019-0481

XVII European Conference
ECSMGE 2019
Reykjavik
on Soil Mechanics
and Geotechnical Engineering

Discrete particle modelling of granular soils using a physics engine
Modélisation discrète des particules des sols granulaires à l'aide d'un moteur physique

H. Li
University of Sheffield, Sheffield, UK

C. C. Smith, P. Shepley
University of Sheffield, Sheffield, UK

ABSTRACT: Physics engines provide an alternative approach to the conventional distinct element method (DEM) for modelling granular soils. Physics engines are software models widely used in computer game and film industries to animate rigid bodies in a physical system. Recent work has shown that the open-source Box2D physics engine is able to successfully capture the critical state response of granular soil media of random polygons simulated in biaxial tests and has a number of advantages over the DEM approach in terms of contact model and particle shape capabilities. In this paper, the application of the technique to biaxial test and retaining wall problems is investigated and the effects of the soil particle geometry and packing characteristics on the small strain and large strain response are examined.

RÉSUMÉ: Les moteurs physiques fournissent une approche alternative à la méthode conventionnelle à éléments distincts (DEM) pour la modélisation des sols granulaires. Les moteurs physiques sont des modèles logiciels largement utilisés dans les industries du jeu vidéo et du cinéma pour animer des corps rigides dans un système physique. Des travaux récents ont montré que le moteur physique open source Box2D est capable de capturer avec succès la réponse à l'état critique des milieux granulaires de polygones aléatoires simulés dans les tests biaxiaux et présente un certain nombre d'avantages par rapport au modèle de contact et à la forme des particules. capacités Dans cet article, l 'application de la technique aux tests biaxiaux et aux problèmes de murs de soutènement est étudiée et les effets de la géométrie des particules du sol et des caractéristiques de tassement sur la petite souche et la grande réponse de la souche sont examinés.

Keywords: Box2D; constraint method; biaxial test; retaining wall; elongated particle; non-elongated particle.

1 INTRODUCTION

The discrete element method is a popular numerical method used in geotechnics to model soil systems at the particle level and to investigate the micro-scale behaviour of granular soils such as internal force networks which are difficult to determine in experiments and conventional continuum models.

A physics engine is computer software widely applied in movies, video games and computer graphics to simulate interactions (or collisions) in physical systems, including rigid bodies, soft bodies and fluid bodies, and there exists some previous work in the literature exploring the application of physics engines to granular soil simulation (Cicekci, Turkeri and Pekcan, 2014; Ehsan and Bezuijen, 2015; Pytlos, Gilbert and Smith, 2015; Xu et al., 2013).

This paper looks at the application of one of the physics engine family, Box2D written by Catto (2005) in C++ to model biaxial tests and retaining wall problems and to study the effects of particle geometry and packing. Box2D is a portable open-source software which has been used to simulate two dimensional rigid bodies and previously applied in digital computer games such as "Angry Bird".

2 ALGORITHMS IN BOX2D

The contact model in Box2D discretises the calculation progress into a number of sub-time schemes. In DEM, the contact model is based on the penalty method, where particles in contact or inter-penetrating are separated in a series of continuous time steps according to the intrusion distance in the corresponding time step; however, the contact model in Box2D depends on the constraint method (or analytical method) (Baraff, 1989; Baraff, 1997; Catto, 2005; Erleben, 2004; Pytlos, Gilbert and Smith, 2015) at the velocity level. A brief introduction is given below.

Two soil particles in relative motion and their potential contacting positions are shown in Figure 1. p_a and p_b are the potential contacting points and $\vec{n}$ is a unit normal vector pointing from particle B to A. The contact conditions can be examined by the separation distance d:

$$d = \vec{n} \cdot (\overrightarrow{p_a} - \overrightarrow{p_b}) \tag{1}$$

If $d > 0$, the particles are separated, while if $d < 0$, the particles should already be inter-penetrating. However, it is hard to justify whether particles are separated or colliding when $d = 0$, in which case the relative velocity v_{rel} is used:

$$v_{rel} = \vec{n} \cdot (\dot{p_a} - \dot{p_b}) \tag{2}$$

where $\dot{p_a}$ and $\dot{p_b}$ are particle vertex velocities and calculated by:

$$\dot{p_a} = v_a + \omega_a \times (p_a - x_a) \tag{3}$$

$$\dot{p_b} = v_b + \omega_b \times (p_b - x_b) \tag{4}$$

where v_a and v_b are translational velocities, ω_a and ω_b are rotational velocities, and x_a and x_b are mass centres. Therefore, for the particles in contact, $v_{rel} > 0$ indicates the particles are moving apart, $v_{rel} < 0$ means particles are colliding and $v_{rel} = 0$ represents particles in rest.

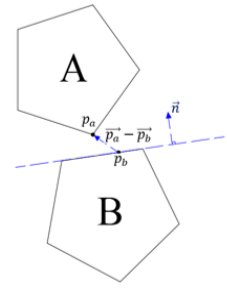


Figure 1. Relative positions between two particles in motion.

For the case of colliding contacts, two impulses J of opposite directions along the unit normal vector $\vec{n}$ will be applied to both particles of mass M in order to make them move apart from each other.

$$J = j \cdot \vec{n} = \Delta v \cdot M \tag{5}$$

If the impulse is applied at the point p, there will be a corresponding torque impulse generated:

$$\tau_{impulse} = (p - x) \times J \tag{6}$$

Thus, the change of angular velocity $\Delta\omega$ is $I^{-1}\tau_{impulse}$, where I is the particle moment of inertia.

Let the prime sign "-" denote the circumstance before the impulse is applied and "+" the condition afterwards. In particular, we need to define a restitution coefficient ϵ between 0 and 1 to give a relation between v_{rel}^{-} and v_{rel}^{+}:

$$v_{rel}^{+} = -\epsilon v_{rel}^{-} \tag{7}$$

ϵ=1 means the particles will separate at the same velocity values as at the colliding step, thus there is no kinetic energy loss and the collision is perfectly elastic, while $\epsilon = 0$ indicates all kinetic energy is lost after colliding.

As defined above, the required impulse J applied to the colliding particles A and B can be calculated respectively.

3 BIAXIAL TEST SIMULATION

Random elongated (ratio of height to width equal to 2) and non-elongated (ratio of height to width equal to 1) soil particles in dense and loose deposits were simulated in a biaxial environment by using Box2D in order to study the influences caused by particle shape and packing characteristics on sand mechanical properties.

To generate the grains, their circumcircles (ABCD and EFGH) were first specified (Figure 2), and then the ratio of height to width (BD/AC and FH/EG) adjusted as appropriate. The other vertices were then set randomly in order to obtain random convex shape.

Sphericity for one particle is defined as the ratio of radius of its inscribed circle to that of its circumscribing circle (Blott and Pye, 2008) and it can describe the degree of elongation. For elongated and non-elongated grains, the average sphericities are 0.62 and 0.81, respectively.

Mechanical parameters including mobilised angle of shearing, void ratio, initial stiffness and contact number were analysed.

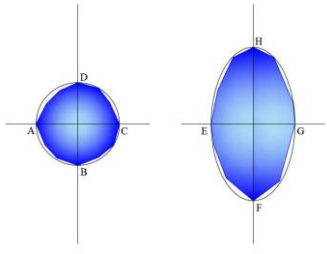


Figure 2. Non-elongated and elongated grains.

3.1 Biaxial model setup

3.1.1 Model parameters

Dense and loose samples of 2000 and 4000 elongated and non-elongated particles were tested in a series of simulations.

The samples were created by setting different initial deposit friction coefficients (0.15 and 0.466) during pluviation while the interparticle friction coefficient was set to 0.466 during the shearing stage. The restitution coefficient was set to 0.2. It was found that this value only has a significant influence on the initial deposition process. A list of the parameters used is given in Table 1.

Table 1. Model setup parameter list.

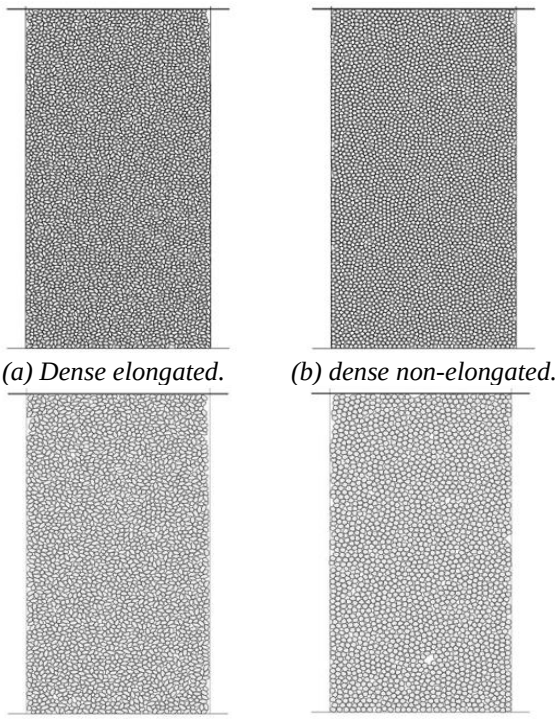
Parameters	Values
Box2D system parameters	
time step size	1/60 s
number of velocity iterations per time step	100
number of position iterations per time step	3
Soil particle and sample characteristics	
restitution coefficient	0.2
Density	2660 kg/m^3
particle width	1.0 m
Test set-up parameters: during generation	
friction coefficient for dense samples	0.15
friction coefficient for loose samples	0.466
gravity acceleration	0.1 m/s^2
Test set-up parameters: during shearing	
friction coefficient of the top cap and the bottom edge	1.0
confining pressure	1000 N/m^2
top cap velocity	0.005 m/s
particle friction coefficient	0.466
gravity acceleration	0 m/s^2

3.1.2 Modelling process

Soil grains were generated at a specific height above the bottom boundary of the biaxial container at time zero and then deposited at a gravity acceleration of $0.1\mathrm{m/s^2}$. After all the particles came to rest, the confining stress was applied using the same process as employed by Pytlos, Gilbert and Smith (2015) and the vertical stress was applied by the strain-control method. Biaxial shearing was continued until the axial strain reached 0.15.

3.2 Biaxial test results

Initial obtained deposits are given in Figure 3 and their final conditions in terms of total rotation at an axial strain of 0.15 are as shown in Figure 4. Obvious shear bands can be observed in both samples. The shear band thickness of the dense non-elongated sample is approximately 10 times particle diameter and 15 times particle diameter for the dense elongated sample, however, shear bands are not that apparent in the loose samples especially in the non-elongated sample.



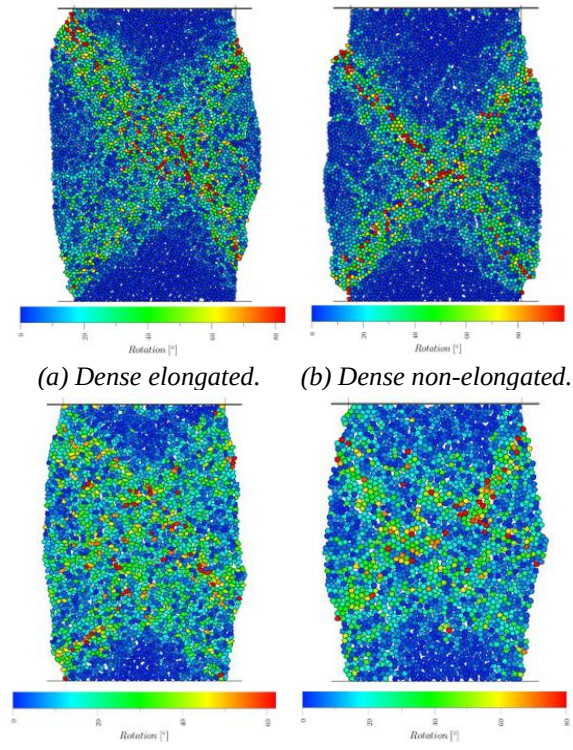
(a) Dense elongated. *(b) dense non-elongated.*

(c) Loose elongated. *(d) Loose non-elongated.*

Figure 3. Initial created samples.

It is also found that the maximum particle total rotation is around 83° and 62° in the dense and loose elongated samples respectively, 15° and 18° smaller than those in the non-elongated sample, indicating that rotation can be inhibited in elongated samples.

The mean coordination number changes are shown in Figure 5. In terms of the dense samples, the values decrease initially, implying dilation continuing, and then stay static after the axial strain reaches around 0.10, while for the loose samples, the mean coordination numbers remain stable during the whole process. The elongated particle samples have larger coordination numbers than the non-elongated ones, therefore, the inter-locking effects influence the elongated



(a) Dense elongated. *(b) Dense non-elongated.*

(c) Loose elongated. *(d) Loose non-elongated.*

Figure 4. Particle rotation at axial strain of 0.15.

particle samples more than non-elongated samples. This also indicates that the rotation of elongated particles has been hampered due to more contacts with adjacent particles.

Very similar results have also been found by Peña et al. (2008). The mean coordination numbers for elongated and non-elongated grains finally oscillate at a mean value of approximately 3.4 and 3.0, respectively.

Alexander (1998) and Edwards (1998) showed that the minimum theoretical mean coordination number is 3 for 2-D frictional granular materials to achieve static equilibium which is in good agreement with the current results of just over 3.

Figure 6 plots the global average void ratio against axial strain. Dilation is observed in the dense samples and the elongated sample shows greater dilatancy than the non-elongated sample. Furthermore, elongated grains are easier to deposit in a loose state compared to non-elongated ones under the same effort. These outcomes coincide well with previous findings (eg. Jensen et al., 2001), which can be explained by rotation being hampered more in elongated samples since particles have larger mean coordination numbers. As a result, the energy dissipation will be mainly by interparticle sliding and dilation, resulting in a larger void ratio.

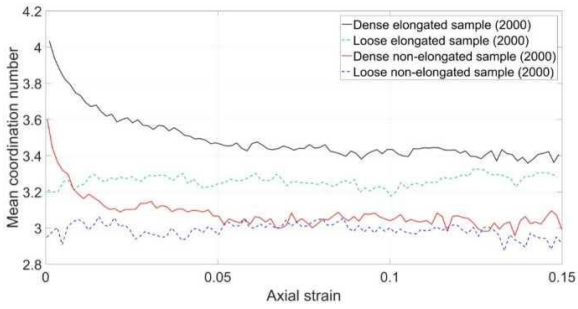


Figure 5. Mean coordination numbers for different particle shapes.

For samples constituted with similar shaped particles but different initial void ratios, the values of the coordination number should be very close at the end of shearing at the critical state as found by Peña (2008). However, because measurements of the mean coordination number and the void ratio are on the global scale instead of within the shear band zone, the values do not converge at the critical state. Further investigation of the detailed shear band processes is in progress.

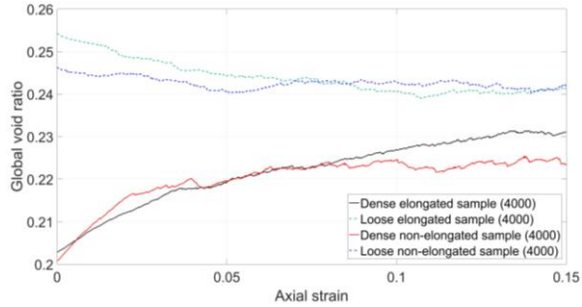


Figure 6. Global void ratio change for different samples.

Figures 7 and 8 compare the mobilised angle of shearing resistance versus axial strain for different particle shapes and numbers of particles modelled.

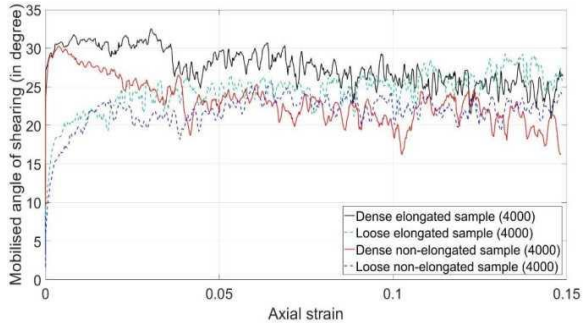


Figure 7. Friction angle versus axial strain for different particle shapes.

The critical friction angles for elongated and non-elongated samples are around 26° and 22°, both irrespective of initial density states (also see Ishihara (1996)). Deposits of elongated particles therefore possess higher shear strength than non-elongated ones (see also Peña, 2008). Our results are slightly lower than those observed by Bardet (1997) in 3-D experiments due to environmental dimension effects. Behaviours of 2000 and 4000

grains agree very well as illustrated in Figure 8, and random conditions do not significantly influence the simulation much, as also demonstrated by Pytlos, Gilbert and Smith (2015).

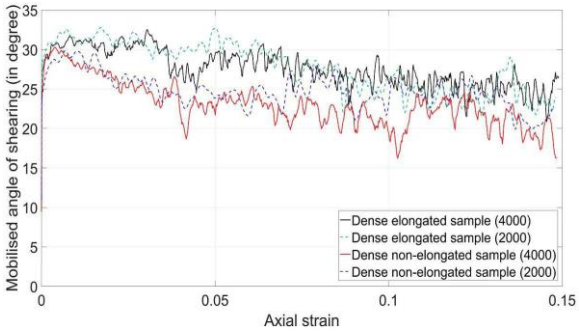


Figure 8. Friction angle versus axial strain for elongated particles but different grain numbers.

Initial stiffness is evaluated by shear modulus, measurable by the slope on the graph plotting deviatoric stress versus deviatoric strain (Figures 9 and 10). The elongated particle samples exhibit higher initial stiffness than the non-elongated particle samples. This may be explained by that elongated particles have higher mean coordination numbers, giving the samples more resistance to deformation.

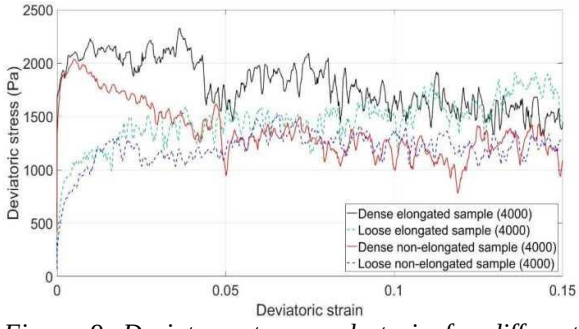


Figure 9. Deviatorc stress and strain for different particle shapes.

Both loose and dense samples show a very stiff response up to a deviatoric strain of around 0.01% and the tangent stiffness then reduces significantly in all samples.

Force chains among contacting particles are shown in Figure 11. The larger axial force chains concentrate at the middle part of the sample along the applied vertical force direction and the values become smaller in the radial direction.

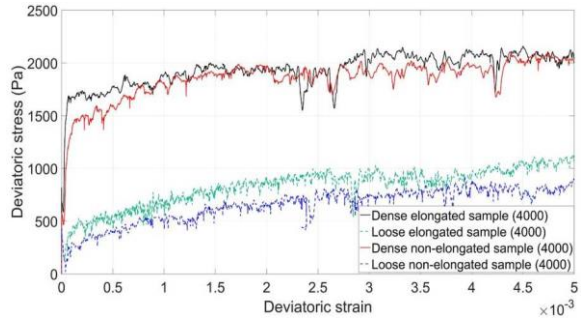


Figure 10. Initial shear modulus for different particle shapes.

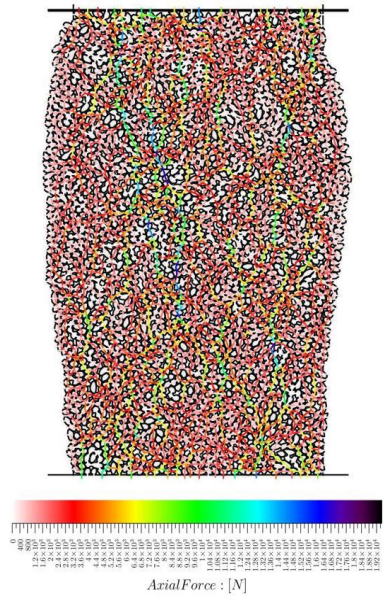


Figure 11. Interparticle normal force chain diagram at axial strain of 10%.

4 RETAINING WALL SIMULATION

4.1 Retaining wall model setup

Both elongated and non-elongated granular soil deposits under passive retaining wall conditions

were simulated in order to determine the influences of particle shape and initial density conditions on passive earth pressure coefficients. The sample preparation process was very similar to that in the bixial simulation. The retaining wall was set to be frictionless and the sample width-to-height ratio was 4 so as to avoid any boundary effects. The numbers of particles for all the models were chosen to be approximately 2000. Other particle parameters were the same as those in the biaxal tests.

4.2 Retaining wall test results

The passive earth pressure coefficient (K_p) can be calculated by equation (8), where P is the lateral contact force between the retaining wall and the deposit, γ and H are the specific gravity and the height of the deposit, ρ_s is the density of the particle and e is the void ratio. Dense elongated and non-elongated particle deposits show very similar peak passive earth pressure coefficients, both around 3, but at different wall movements to reach this value as Figure 12 shows. In the critical state, after ratio of wall movement to initial deposit height reaches about 0.6, both dense and loose deposits filled with elongated grains exhibit higher K_p against the non-elongated granular deposits. K_p of the elongated particle deposits in the critical state is in the neighbourhood of 2.6 while 2.2 for the non-elongated ones, indicating the initial density conditions do not influence the final critical state. According to Rankine theory, when the wall is assumed to be frictionless and the backfill inclined angle is zero, K_p can be calculated by equation (9).

$$K_p = \frac{2P}{\gamma H^2} = \frac{2(1+e)P}{\rho_s g H^2} \quad (8)$$

$$K_p = \frac{1+\sin\phi}{1-\sin\phi} \quad (9)$$

ϕ is particle friction angle at the critical state and $26°$ for elongated samples and $22°$ for non-elongated samples in this simulation. Therefore, K_p should be 2.56 and 2.20 for two different samples as calculated and our results agree well with the analytical values.

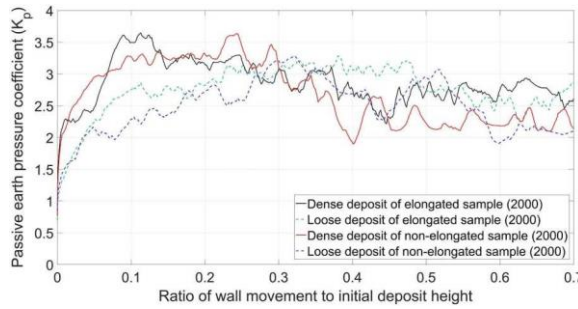
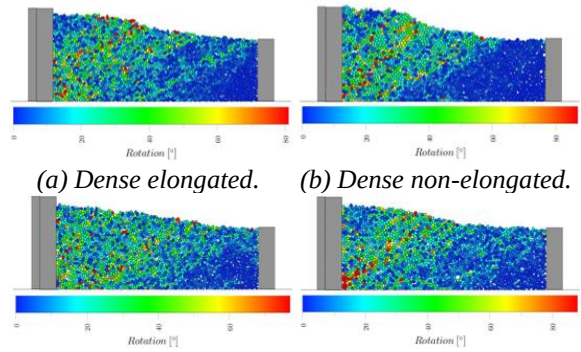


Figure 12. Passive earth pressure coefficients in terms of various packings.

Figure 13 shows the particle rotation for the dense and loose deposits of the retaining wall model at the ratio of wall movement to initial deposit height equal to 0.7. Shear banding is more apparent in the dense samples, and the maximum total rotation angles for the dense and loose non-elongated particle samples are 6° and 10° higher than those for the dense and loose elongated particle samples respectively.



(a) Dense elongated. *(b) Dense non-elongated.*

(c) Loose elongated. *(d) Loose non-elongated.*

Figure 13. Particle rotation for samples of retaining walls.

5 CONCLUSIONS

Biaxial test and retaining wall simulations were both implemented via Box2D in this research to

study the influences on granular soil behaviour in terms of elongated and non-elongated particles.

The results show that Box2D can successfully model shear bands and determine particle force chains elucidating granular soil micro-mechanical behaviour.

In the biaxial test simulations, elongated particle samples were found to have larger mean coordination numbers, greater dilatancy, higher friction angles and stiffnesses than non-elongated particle samples. The elongated particle samples exhibit nearly 8% and 18% higher peak and critical mobilised shearing angles compared to the non-elongated particle samples. As expected, the initial sample density condition does not influence the critical state properties.

In the retaining wall simulation, elongated particle deposits give around 18% higher critical passive earth pressure coefficient values.

6 REFERENCES

Alexander, S., 1998. Amorphous solids: their structure, lattice dynamics and elasticity. Physics reports, 296(2-4), pp.65-236.

Bardet, J.P., 1997. Experimental soil mechanics. Prentice Hall.

Baraff, D., 1989, July. Analytical methods for dynamic simulation of non-penetrating rigid bodies. In ACM SIGGRAPH Computer Graphics (Vol. 23, No. 3, pp. 223-232). ACM.

Baraff, D., 1997. An introduction to physically based modeling: rigid body simulation II—nonpenetration constraints. SIGGRAPH course notes, pp.D31-D68.

Blott, S.J. and Pye, K., 2008. Particle shape: a review and new methods of characterization and classification. Sedimentology, 55(1), pp.31-63.

Catto, E., 2005, February. Iterative dynamics with temporal coherence. In Game developer conference (Vol. 2, No. 4, p. 5).

Cicekci, O.C., Turkeri, M.K. and Pekcan, O., 2014. Development of Soil Profile Visualization Software Using Game Engines. In *Geo-Congress 2014: Geo-characterization and Modeling for Sustainability* (pp. 3364-3372).

Edwards, S.F., 1998. The equations of stress in a granular material. Physica A: Statistical Mechanics and its Applications, 249(1-4), pp.226-231.

Ehsan, I. and Bezuijen, A., 2015. Simulation of granular soil behaviour using the bullet physics library. In *3rd International Symposium on Geomechanics from Micro to Macro* (Vol. 2, pp. 1565-1570). Taylor and Francis Group-London.

Erleben, K., 2004. Stable, robust, and versatile multibody dynamics animation. Unpublished Ph. D. Thesis, University of Copenhagen, Copenhagen.

Jensen, R.P., Edil, T.B., Bosscher, P.J., Plesha, M.E. and Kahla, N.B., 2001. Effect of particle shape on interface behavior of DEM-simulated granular materials. International Journal of Geomechanics, 1(1), pp.1-19.

Peña, A.A., 2008. Influence of particle shape on the global mechanical response of granular packings: Micromechanical investigation of the critical state in soil mechanics (Doctoral dissertation, Ph. D. thesis, ISBN: 978-3-921837-59-7, University of Stuttgart, Germany).

Pytlos, M., Gilbert, M. and Smith, C.C., 2015. Modelling granular soil behaviour using a physics engine. *Géotechnique Letters*, *5*(4), pp.243-249.

Xu, Z., Lu, X., Guan, H. and Ren, A., 2013. Physics engine-driven visualization of deactivated elements and its application in bridge collapse simulation. *Automation in Construction*, *35*, pp.471-481.